Large-eddy simulation of turbulent gas-particle flows in the duct induced by the wall injection

K.N. Volkov*

School of Engineering, University of Surrey, Guildford, GU2 7XH, UK

Abstract

Turbulent gas-particle flows in the duct with fluid injection are simulated using large-eddy simulation technique. The numerical calculations are performed by the Eulerian-Lagrangian approach for the fluid and solid phases respectively. The model developed of motion of particles takes into account fluctuations of fluid velocity. The influence of inflow conditions, and the size and place of injection of particles on their dispersion pattern are investigated. The results obtained have a good agreement with the results computed on the base of Reynolds averaged Navier-Stokes equations and experimental data.

Keywords: Two-phase flow; Turbulence; Large-eddy simulation; Computational fluid dynamics; Internal flow

1. Introduction

Gas-particle flow research has applications to a vast number of technological systems and industrial devices. In technological applications the interaction of the particles with the turbulent structure of the flow is an extremely complex problem. The introduction of new models and improved computer power allows making more accurate computations performed with less empiricism than before.

The large-eddy simulation (LES) of internal turbulent flows induced by wall injection is considered in the paper. Simulation of such flows is of great significance for the design of heat exchangers and solid rocket motors. In these applications, exact computation of field of fluid flow plays an important role because it serves as a background for simulation of condensed particles formed during the combustion of solid fuel, their interaction and separation on a wall [1,2]. The purpose of calculations employed is in the definition of optimal initial parameters of duct flow and lead-in conditions of solid particles.

* Tel.: +44 (1483) 683222; E-mail: k.volkov@surrey.ac.uk

Computational Fluid and Solid Mechanics 2005
K.J. Bathe (Editor)

2. Mathematical model and numerical method

The numerical calculations are performed by the Eulerian-Lagrangian approach for the fluid and solid phases respectively.

2.1. Basic assumptions

It is assumed that the particles are rigid spheres, there are no particle–particle interactions, the density of the dispersed phase is much more than the density of the gas phase, the dominant force acting on the particle is the drag force, and the influence of the particle phase on the carrying gas is negligible.

2.2. Gas phase

The fluid flow calculations are based on the filtered Navier-Stokes equations:

$$\frac{\partial \tilde{v}_j}{\partial x_j} = 0 \tag{1}$$

$$\frac{\partial \tilde{v}_i}{\partial t} + \frac{\partial \tilde{v}_i \tilde{v}_j}{\partial x_j} = -\frac{1}{\rho}\frac{\partial \bar{p}}{\partial x_i} + \frac{\partial}{\partial x_j}\left[(\tilde{\nu} + \nu_t) + \frac{\partial \tilde{v}_i}{\partial x_j}\right] \tag{2}$$

where ρ, p, v, ν are the density, the pressure, the velocity and the kinematic viscosity. Sub-grid turbulent viscosity is computed with the Smagorinsky formula:

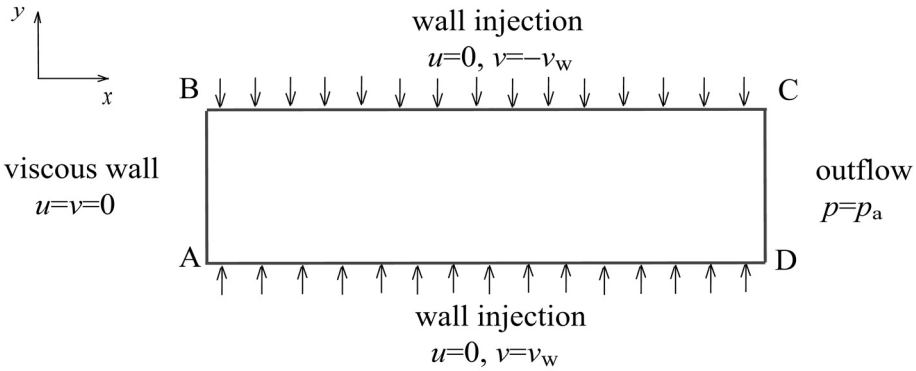

Fig. 1. Geometry of computational domain.

$$\nu_t = (C_S\Delta)^2|\tilde{\varepsilon}|, \quad |\tilde{\varepsilon}| = (2\tilde{\varepsilon}_{ij}\tilde{\varepsilon}_{ij})^{1/2}, \quad \tilde{\varepsilon} = \frac{1}{2}\left(\frac{\partial\tilde{v}_i}{\partial x_j} + \frac{\partial\tilde{v}_j}{\partial x_i}\right)$$

where C_S is the Smagorinsky constant. The sub-grid length is assumed to be proportional to the filter width, which then is related to the volume of grid mesh in three dimensions:

$$\Delta = (\Delta x \Delta y \Delta z)^{1/3}$$

where Δx, Δy, Δz are the grid step size in the corresponding coordinate direction. The present LES calculations implicitly apply a box filter in each direction.

The geometry of computational domain is shown in Fig. 1 (side view). The left boundary of a duct is a solid wall, and no-slip boundary conditions are set here. The outflow boundary conditions are used on the outlet boundary. The injection of fluid at normal to the lateral surface of a duct is set (wall injection). The velocity of fluid injection is constant along the longitudinal coordinate.

2.3. Solid phase

The solid phase is treated by the Lagrangian approach, which means that particles are followed in time along their trajectories through the flow field. The equations describing the translational motion of spherical particles are written as

$$\frac{d\boldsymbol{r}_p}{dt} = \boldsymbol{v}_p \tag{3}$$

$$\frac{d\boldsymbol{v}_p}{dt} = \frac{3C_D\times\rho}{8\rho_p r_p}|\boldsymbol{v} - \boldsymbol{v}_p|(\boldsymbol{v} - \boldsymbol{v}_p) \tag{4}$$

The drag coefficient is presented in the following form:

$$C_D = \frac{24}{Re_p} f_D(Re_p), \quad f_D(Re_p) = (1 + 0.179Re_p^{0.5} + 0.013Re_p)$$

where

$$Re_p = \frac{2r_p|\boldsymbol{v} - \boldsymbol{v}_p|}{\nu}$$

At every given time step, the new position and the new translational velocity of the particles are calculated according to the forces acting on the particles. LES allows fluctuating components to be obtained spontaneously from Eqs (3) and (4), unlike approach [1,3], which uses normal distribution for fluctuating properties of internal turbulent flow.

2.4. Numerical method

The filtered equations are solved numerically using a finite volume method on a staggered grid of non-uniform cell size.

The numerical procedure employs a Chorin-type projection method for the decoupling of momentum and continuity equations. The second-order explicit Adams-Bashforth time integration scheme is used to advance the velocity field. The discretisation of the diffusive flux is based on the central differences of second order of accuracy. The sharp and monotonic algorithm for relative transport (SMART) is used to calculate the convective fluxes [4]. The Poisson equation for pressure is solved by the bi-conjugate gradients stabilised method (BiCGStab) with preconditioning [5].

2.5. Parallelisation

The computational domain is divided into several rectangular sub-domains. Each process holds some ghost cells, which overlap inner cells of the adjacent process. Values are copied from these to the ghost cells when necessary. To minimise communications, the code divides the computational domain in a way that minimises the area of the touching faces and equilibrates the

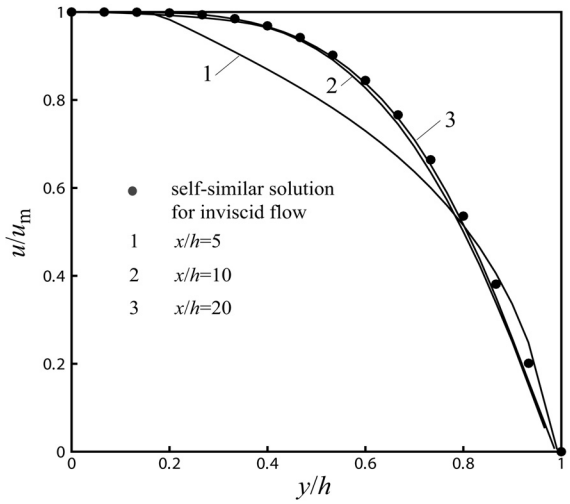

Fig. 2. Profiles of longitudinal velocity. Comparison with self-similar solution.

number of cells in the different sub-domains. The MPI library is used for organisation of communication between processors.

2.6. Results

A grid containing 100 × 100 cells in the duct cross section and 300 sections downstream is used in a typical variant of the calculation. The time step size is Δt = 0.000018 s. About 50000 time steps are done. To obtain a statistically reliable averaged pattern of motion of particles about 30000 particles are tracked.

Fluid flow pattern was investigated depending on intensity of fluid injection and Reynolds number Re = $v_w h/\nu$, where v_w is the velocity of fluid injection, and h is the half-width of the duct. The computed results are compared with the approximate solutions, the available benchmark solutions and experimental data.

The problem has a self-similar solution for inviscid flow of incompressible fluid. The profiles of the velocity in the x and y directions are defined by the following expressions [6,7]:

$$\frac{u}{v_w} = \frac{\pi x}{2h}\cos\left(\frac{\pi y}{2h}\right), \quad \frac{v}{v_w} = -\sin\left(\frac{\pi y}{2h}\right)$$

Fig. 2 shows profiles of axial velocity in some cross sections of a duct. The velocity of fluid injection is v_w = −5 m/s. The results obtained have a good agreement with a self-similar solution. Also, the flow becomes fully developed some distance from the left boundary, and the axial velocity profiles are practically identical. Viscous effects do not influence the flow structure in a duct. Therefore, the inviscid solution can be used for comparison with calculation results in the viscous case. For example, the longitudinal velocity has linear dependence along its x-coordinate, and the profile of the lateral velocity does not depend on the x-coordinate, and has a universal form.

The results obtained show that the level of turbulence can be computed in two steps. The first step is the calculation of the velocity field without any turbulence model using the Euler or Navier-Stokes equations. The second step is the solution of the equations of the turbulence model. The difference has a place far from between the solution of the coupled problem and developed step-by-step solution is located at $x/h > 30$, and it can be explained by the compressibility effects.

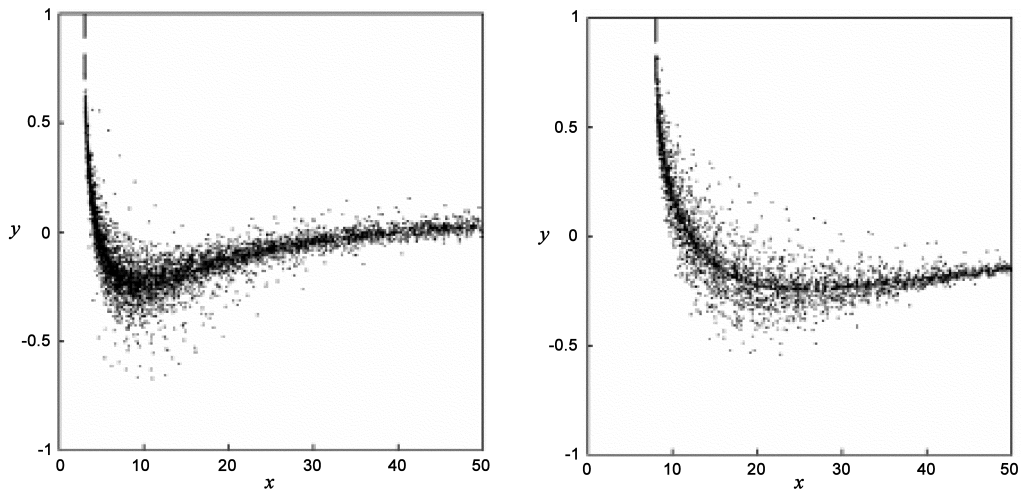

Fig. 3. Pattern of particle dispersion for r_p = 10 μm.

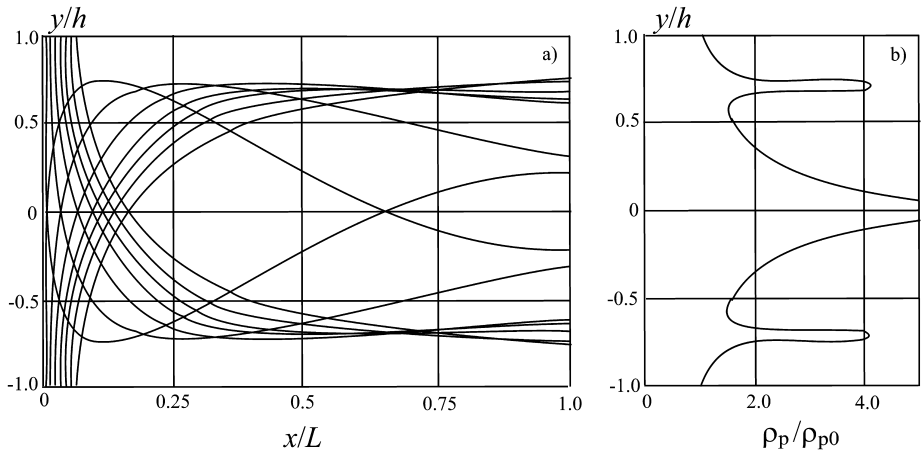

Fig. 4. Trajectories of particles (left) and profile of concentration of particles (right) in the duct for $r_p = 20\,\mu$m.

The distribution of turbulence kinetic energy along the x-coordinate has a parabolic form [8], and the distribution of its dissipation rate has a cubic dependence against the x-coordinate, excluding the region near the left boundary where the flow is not fully developed. It is also confirmed by the results obtained on the base full 3D model [1,2].

The dispersion of particles is defined by the relation of the particle relaxation time to the dissipation dynamic time scale of the turbulence. The particles with radius $r_p < 10\,\mu$m hit a target in the region with a maximum value of fluid velocity turbulent fluctuations. Such particles are dispersed strongly (see Fig. 3). The region of increased particle concentration is formed in the vicinity of the centreline of the duct. Inert particles penetrate to the opposite wall, where the turbulence level is equal to zero, and are not dispersed. The regions of irregular particle concentration are formed near the separatrixes of trajectories of particles (see Fig. 4).

3. Conclusions

The simulation of internal flow induced by the wall injection shows that velocity fluctuations exercise an essential influence on the dispersion of particles. The results obtained have a good agreement with the results computed on the base of Reynolds-averaged Navier-Stokes equations and experimental data. The models developed reasonably explain computational and experimental data. In particular, they explain the formation of regions of irregular particle concentration in the internal duct flow with fluid injection.

Successful application of LES for calculation of properties of internal turbulent flows makes possible calculations taking into account more complex physical and chemical effects. It requires development of sub-grid scale models for compressible fluids, a connection combustion model and the elaboration of corresponding computational tools.

References

[1] Volkov KN, Emelyanov VN. Stochastical model of condensed particle motion in the duct with fluid injection. Math Simulation 1999;11(3):105–111.
[2] Volkov KN, Emelyanov VN. Three-dimensional flows in the ducts with fluid injection. In: Modern Problems of Non-equilibrium Gas and Thermodynamics. Saint Petersburg: BSTU, 2002.
[3] Gosman AD, Ioannides E. Aspects of computer simulation of liquid-fueled combustors. AIAA Paper 81–0323.
[4] Choi SK, Nam HY, Cho M. A comparison of higher-order bounded convection schemes. Comput Methods Appl Mech Eng 1995;121:281–301.
[5] Van der Vorst HA. Bi-CGSTAB: A fast and smoothly conversing variant of Bi-CG for the solution of non-symmetric linear systems. SIAM J Sci Stat Comput 1992;13:631–644.
[6] Olson RM, Eckert ERG. Experimental studies of turbulent flow in a porous circular tube with uniform fluid injection through the tube wall. J Appl Mech 1966;33(1):82–88.
[7] Pennel WT, Eckert ERG, Sparrow EM. Laminarization of turbulent pipe flow by fluid injection. J Fluid Mech 1972;52(3):451–464.
[8] Spiridonov FF. Distribution of turbulence quantities in the duct with intensity fluid injection. J Theor Appl Mech 1987;5:79–84.